SCIENTIFIC REPORTS
nature research

OPEN

A density functional theory study of high-performance pre-lithiated MS_2 (M = Mo, W, V) Monolayers as the Anode Material of Lithium Ion Batteries

Tingfeng Liu[1], Zhong Jin[2,3], Dong-Xin Liu[4], Chunmiao Du[1], Lu Wang[1], Haiping Lin[1]✉ & Youyong Li[1]✉

Recent experimental study shows that the pre-lithiated MoS_2 monolayer exhibits an enhanced electrochemical performance, coulombic efficiency of which is 26% higher than the pristine MoS_2 based anode. The underlying mechanism of such significant enhancement, however, has not yet been addressed. By means of density functional theory (DFT) calculations, we systematically investigated the adsorption and diffusion behavior of lithium (Li) atoms on the MS_2 (M = Mo, W, V) monolayers. On the pre-lithiated MS_2 monolayers, the adsorption energy of extra Li ions are not significantly changed, implying the feasibility of multilayer adsorption. Of importance, the Li diffusion barriers on pre-lithiated MS_2 are negligibly small because of the charge accumulation between the diffusing Li ions and the pre-lithiating Li layer. Correspondingly, we report that the pre-lithiation should be a general treatment which can be employed on many transition-metal di-chalcogenides to improve their storage capacities and charge-discharge performance in Li ion batteries. In addition, we propose that the pre-lithiated VS_2 may serve as an outstanding anode material in LIBs.

The Lithium-ion battery (LIB) has been regarded as one of the most indispensable and promising devices in the fields of telecommunications, electric automobiles and electric power grids[1,2]. Today, graphite is widely used as the anode material of commercial LIBs owing to its layered structure, good electric conductance and excellent chemical stabilities[3,4]. Nevertheless, the maximum specific capacity of lithium ions of graphite (LiC_6) is only 372 $mA{\cdot}h{\cdot}g^{-1}$. As a result, numerous researches have been devoted to the searches of new anode materials with higher energy densities[1,5–7]. In addition to the specific capacity, columbic efficiency has also been employed to evaluate the performance of electrodes in LIBs. Thus, an ideal anode material, should not only accommodate densely packed Li ions, but also allow for fast Li diffusions to promote the charge-discharge rate[1,8–10]. In the past decade, a number of two-dimensional (2D) materials, including transition-metal oxides, di-chalcogenides (MO_2 and MS_2) and BN, have been successfully synthesized[11–13]. Their electronics properties and potential applications in devices have also been explored and proposed as electrode material for LIBs[14–20]. Very recently, Yang *et al.* report that the coulombic efficiency of MoS_2 can be significantly improved by the pre-lithiation treatment, in which the MoS_2 is on direct contact with lithium foils[21]. Despite the improved performance of MoS_2 upon pre-lithiation, the underlying mechanism however, has not yet been addressed. Herein, systematic Density Functional Theory (DFT) calculations have been conducted to explore (i) the chemical insights of the enhanced performance after pre-lithiathion, and (ii) the effect of pre-lithiathion on other MS_2 nanosheets. Our results revealed that the pre-lithiathion allows for multilayer adsorption and fast diffusion of Li ions on the MS_2. In addition, pre-lithiathion may serve as a general treatment for improving the performance of MS_2 anode in LIB.

[1]Institute of Functional Nano & Soft Materials (FUNSOM), Jiangsu Key Laboratory for Carbon-Based Functional Materials & Devices, Soochow University, 199 Ren'ai Road, Suzhou, 215123, Jiangsu, P.R. China. [2]Computer Network Information Center, Chinese Academy of Sciences, Beijing, 100190, China. [3]Center of Scientific Computing Applications & Research, Chinese Academy of Sciences, Beijing, 100190, China. [4]Jinduicheng Molybdenum Co. Ltd., No. 88 Jinye 1st Road, High-tech Zone Xi'an, Shanxi, P.R. China. ✉e-mail: hplin@suda.edu.cn; yyli@suda.edu.cn

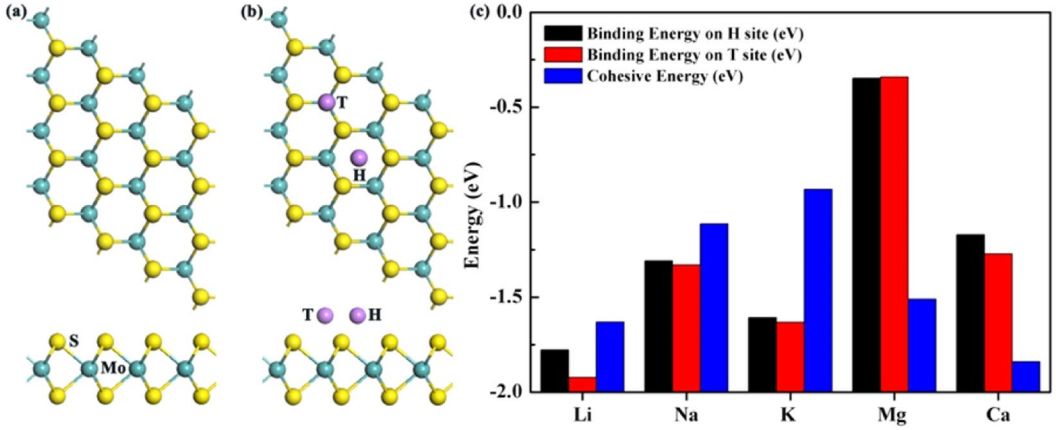

Figure 1. The top and side views of the optimized structures of (**a**) a MoS_2 monolayer and (**b**) the top (T) and hollow (H) binding sites of a metal ion adsorbed on the MoS_2 monolayer. The Mo atoms, S atoms and the binding sites are represented with green, yellow and purple circles, respectively. (**c**) The binding energies and metal cohesive energies of Li, Na, K, Mg, Ca on MoS_2.

Last but not least, the VS_2 monolayer provides relatively high Li binding strength, negligibly small Li diffusion barriers, and large theoretical capacity comparing with MoS_2 and WS_2 counterparts. We thus propose that the pre-lithiated VS_2 monolayer is an outstanding anode material for LIBs. These results may open up a new avenue for the development of the next-generation high-performance LIBs.

Computational Details

The DFT calculations were carried out with the Vienna ab-initio Simulation Package (VASP) code[22–25]. The projector augmented-wave potentials (PAW)[26] and the Perdew–Burke–Ernzerhof (PBE) generalized gradient approximation (GGA) functional[25,27] were used to describe the electron–ion interactions and electronic exchange correlations, respectively. The effect of on-site Coulomb interactions on the binding of Li ions on the MoS_2, $MoSe_2$, WS_2 and WSe_2 have been investigated by previous theatrical studies[28]. It was shown that the binding energy, binding height and diffusion barriers of Li ions are not significantly affected by the on-site Coulomb interactions. Correspondingly, the PBE functional was selected in this work. The conjugate gradient scheme was used to relax all atomic positions and lattice constants until the components of the forces on each atom is of the order of 10^{-3} eV Å^{-1}. A plane-wave basis set with kinetic energy cutoff is set as 500 eV to ensure the accuracy of the simulation results. The number of K-mesh was ($16 \times 16 \times 1$) for the primitive MS_2 unit cell and scaled according to the size of the supercells in the total energy and self-consistent-field (SCF) potential calculations. Based on the primitive cell (1×1), different supercells including (2×1), (2×2), (3×3), and (4×4), hexagonal structures as the ideal models are used to analyze the adsorption of lithium. The corresponding Brillouin zones of the (2×1), (2×2), (3×3), and (4×4) supercells are sampled with the Γ-centered k-point grid of $9 \times 9 \times 1$, $8 \times 8 \times 1$, $6 \times 6 \times 1$, and $2 \times 2 \times 1$, respectively. The lattice constants of MoS_2 (3.186 Å), WS_2 (3.186 Å) and VS_2 (3.236 Å) were obtained from our DFT calculations. These lattice constants are in good agreement with the experimental values[29–33]. A vacuum of 20 Å along the z-axis was applied to prevent interlayer interactions from transnationally periodic images. The Climbing Image Nudged Elastic Band (CI-NEB) method was used to find the saddle points and minimum energy paths between the initial and final states[34–36].

Results and Discussion

In two-dimensional transition-metal di-chalcogenides, the atomic layer of metal elements are sandwiched between two S layers. As shown in Fig. 1(a), the Mo−S bond length of the 2H-MoS_2 is 2.41 Å, and the Mo−S − Mo bond angle is 80.68°, agreeing well the previous theoretical results[37]. Two binding sites are considered for analyzing the adsorption of Li ions on the MoS_2. The top site (T site) is directly above one Mo atom, while the hollow site (H site) is above the center of a hexagon, as shown in Fig. 1(b). We have also examined the other possible adsorption sites (e.g. above the S atom), however, the adsorbed Li ion is observed to move to the neighboring T site after structural relaxation. The binding energy of metal atoms on the MS_2 is defined as:

$$E_b = \left(E_{nLi-MS_2} - nE_{Li} - E_{MS_2}\right)/n \quad (1)$$

The $E_{nLi\text{-}MS2}$ is the total energy of the coupled structure, in which n Li ions adsorbing on the MS_2. E_{Li} is the energy of an isolated Li atom in a vacuum. E_{MS2} is the energy of an isolated MS_2 monolayer. And n is the number of adsorbed Li atoms. According to such definition, a more negative binding energy indicates a more favorable exothermic interaction between MS_2 and Li atoms. As shown in Fig. 1, the adsorption of a Li ion at the T site (−1.94 eV) is more stable than that on the H site (−1.78 eV), with a Li-S distance being 2.37 Å, consisting well with previous theoretical studies[28,37]. In addition to Li ions, the adsorption of other metal elements which possess potential barrier applications have also been calculated. The binding energies of different adsorbing atoms and their corresponding cohesive energies are shown in Fig. 1(c). It can be seen that the binding of Li, Na and K atoms

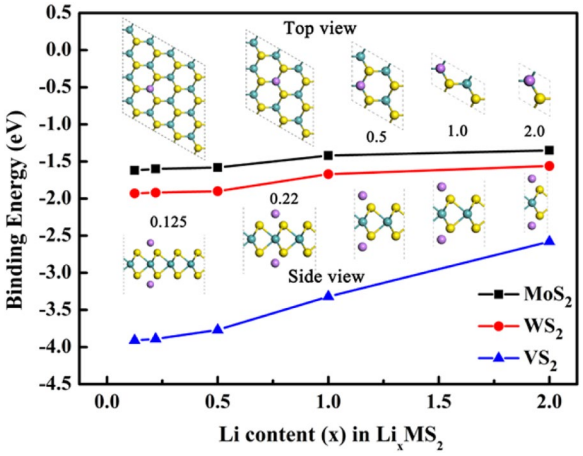

Figure 2. The top and side views of Li_xMS_2 and their averaged Li binding energies on MS_2 monolayers.

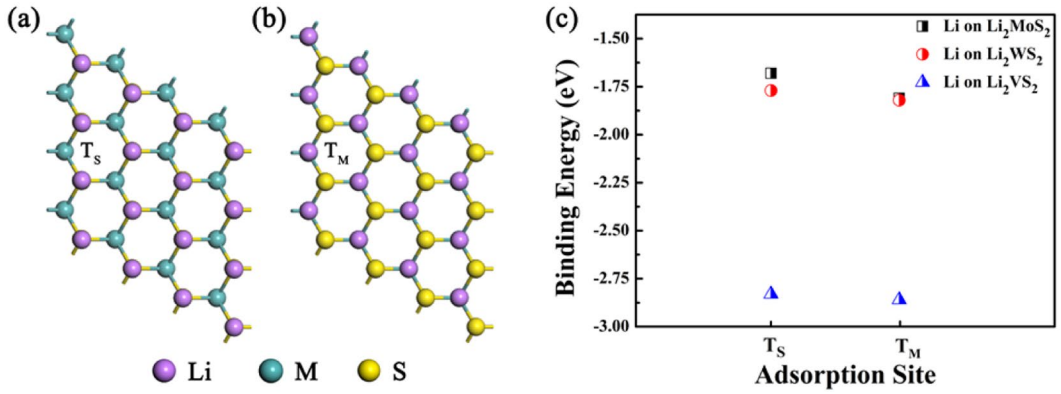

Figure 3. The top and side views of the pre-lithiated MS_2 monolayer (M = Mo, W, V), with one Li atom adsorbing (**a**) above the S atoms (T_S site) and (**b**) above each metal atoms (T_M site). (**c**) The binding energies of a full coverage of Li atoms adsorbing on MS_2 monolayers at the T_S and T_M sites.

on MoS_2 are stronger than the metallic bonds in their bulk structures. This suggests that the MoS_2 may also be employed as anode materials for Na and K ion batteries.

Subsequently, the Li storage capacities of MS_2 monolayer (M = Mo, W, V) were investigated. A series of Li/MS_2 configurations with different stoichiometry of $LixMS_2$ (x = 0.125, 0.222, 0.500, 1.000, and 2.000) were constructed by adding one Li ion on each side of the (4 × 4), (3 × 3), (2 × 2), (2 × 1) and (1 × 1) supercells, respectively. As shown in Fig. 2, the binding energies of Li ions decreases with increasing Li coverages. It is worthy to note that the Li binding energies on VS_2 are much larger than on other MS_2. When x = 2, full Li coverages are achieved on both sides of MS_2. It is seen that the averaged binding energies of Li ions on fully covered VS_2, MoS_2 and WS_2 are −2.58 eV, −1.35 eV and −1.56 eV, respectively. This indicates strong attractive interactions between Li ions and MS_2 monolayers at the full coverage.

The Li_2MS_2 represents the highest Li storage capacity on bare MS_2. At this coverage, the theoretical capacity can be calculated with the following equation:

$$C = cnF/M_{MS_2} \tag{2}$$

here c is the number of adsorbed cations on a MS_2 unit and n is the valence state of fully ionized cations from electrolyte, F is the Faraday constant (26801 mA·h·mol^{-1}), and M_{MS_2} the molar weight of MS_2. In this case, c is 2 at the full coverage, and n is 1for Li ions. Correspondingly, for the adsorption capacities are 334.87, 256.49 and 465 mA·h·g^{-1} for the pristine MoS_2, WS_2 and VS_2 monolayers, respectively.

Previous experimental studies show that the pre-lithiated MoS_2 monolayer exhibit better performance compared with the pristine MoS_2[21]. In order to obtain an in-depth understanding, the adsorption and diffusion of extra Li atoms on the pre-lithiated MS_2 are investigated. Firstly, as shown in Fig. 3, two possible pre-lithiated configurations have been considered, the layered Li atoms prefer to adsorb above the T_M site of the MS_2 monolayer with the binding energies being −1.81 eV (MoS_2), −1.82 eV (WS_2), and −2.86 eV (VS_2), respectively. The corresponding Li-S distances are 2.45 Å (MoS_2), 2.51 Å (WS_2) and 2.32 Å (VS_2).

Figure 4 shows the configurations and corresponding binding energies of extra Li atoms adsorbing the pre-lithiated VS_2 (Li_2VS_2) monolayer with various coverages. As seen, the binding energies of the Li ions on

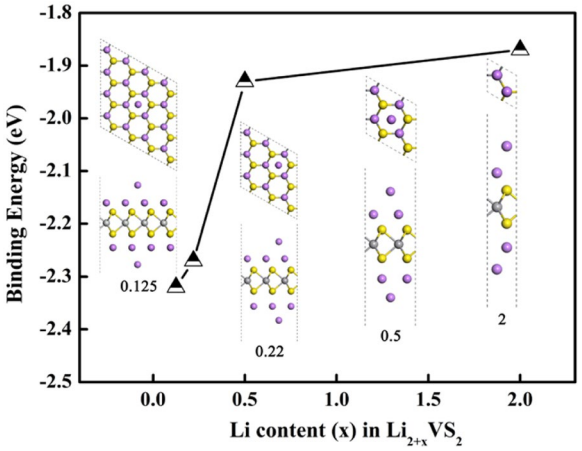

Figure 4. The trends of the binding energies of the Li ion adsorbing on the pre-lithiated VS_2 (Li_2VS_2) with increasing Li coverages.

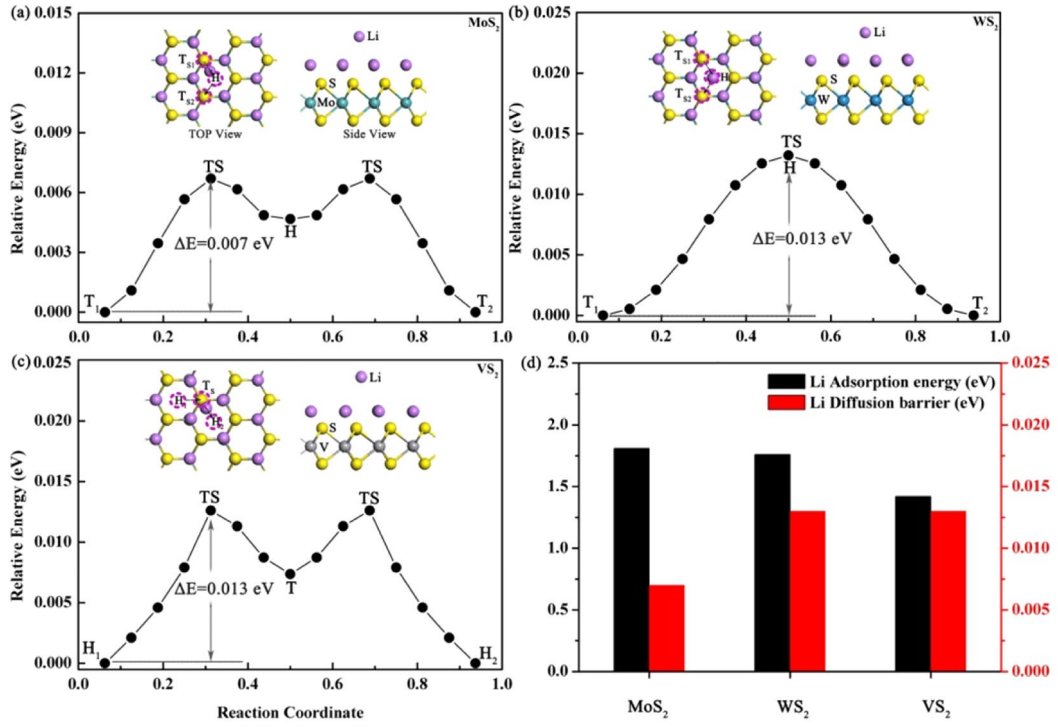

Figure 5. The energy profiles of Li diffusion on the pre-lithiated (**a**) MoS_2, (**b**)WS_2, and (**c**)VS_2. (**d**) The Li binding energy at T site and diffusion barriers.

Li_2VS_2 monolayer decreases gradually with the elevation of the related storage ratio (x). On the pre-lithiated VS_2, the Li ions used for pre-lithiation are assumed anchored on the VS_2 and thus the Li storage capacity is defined as:

$$C = cnF/M_{Li_2MS_2} \quad (3)$$

maximum theoretical capacity of the Li atoms on the pre-lithiated MS_2 (M = Mo, W, V) monolayers were 308.14, 204.70 and 415.67 $mA{\cdot}h{\cdot}g^{-1}$ respectively. Thus, from the point of the binding energy and the theoretical capacity, Li_2VS_2 is relatively more suitable for LIBs anode materials for the higher binding energy and theoretical storage capacity.

The performance of an electrode material is closely related the mobility of the adsorbed Li ions[38]. In general, a lower diffusion barrier means a higher diffusion rate[39,40]. Thus it is necessary to study the diffusion behavior Li ions when the Li_2MS_2 monolayers are used as the substrates. The migrations of the Li atom among the T site and the H site are studied using the CI-NEB method. The red circles and black arrows in Fig. 5 represent the diffusion pathway of the Li atom from the most stable adsorption site (T site or H site) to the next equivalent

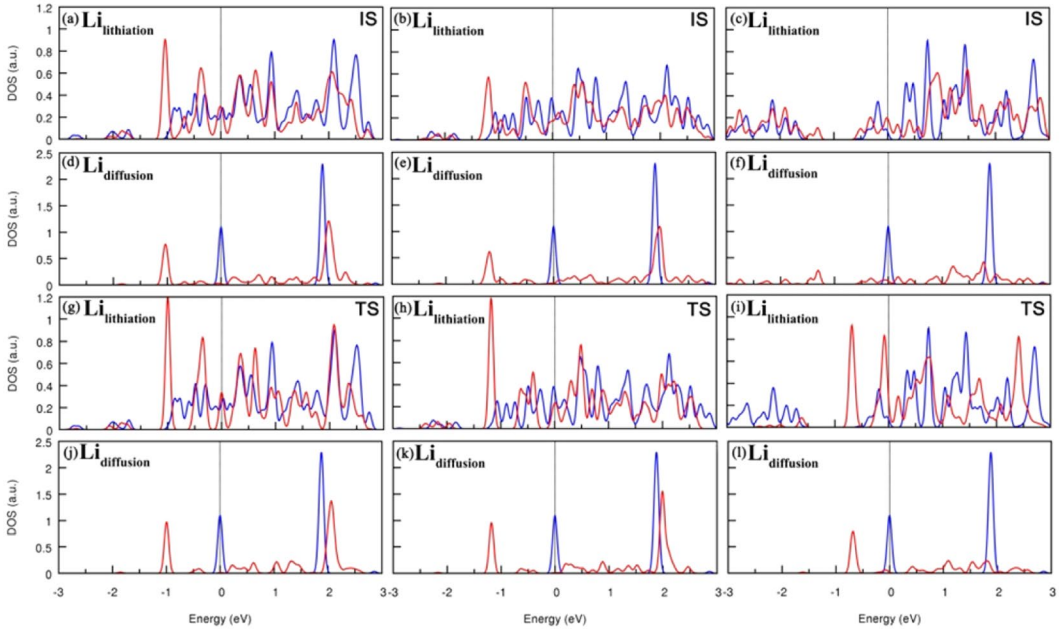

Figure 6. The corresponding local densities of states (LDOS) of the initial states (IS) and transition states (TS) of Li diffusion on Li_2MS_2 monolayers. (**a–c**) are the LDOS of the pre-lithiated Li atoms with (blue curve) and without (red curve) an additionally adsorbed Li atom. (**d–f**) are the LDOS of a Li atom in the vacuum (blue curve) and on the Li_2MS_2 surfaces (red curve) of the IS structures. (**g–i**) and (**j–l**) are the LDOS of corresponding Li ions of the transition states.

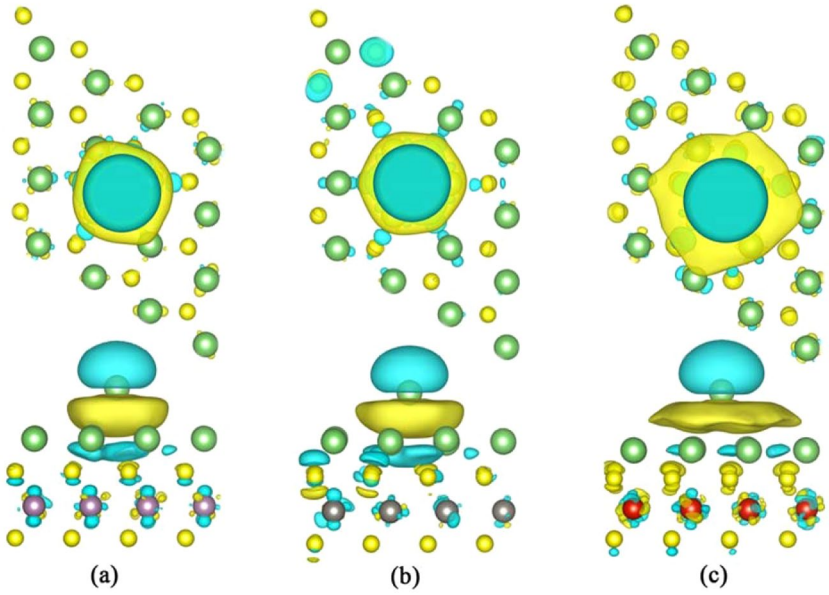

Figure 7. The top and side views of the differential charge densities of the transition states of the diffusing Li atom on the (**a**) Li_2MoS_2, (**b**) Li_2WS_2 and (**c**) Li_2VS_2 monolayers. The light blue and yellow contours (isosurface = 0.001 e/Å^3) represent the charge deletion and charge aggregation, respectively.

stable adsorption site. As seen in Fig. 5(a–c), when Li ions only need to overcome very small energy barriers to diffuse on the pre-lithiated MS_2. Taking into account that the Li diffusion barriers in graphite (0.22 eV) and the pristine MS_2 (0.22 eV) (M = Mo, W, V) are much higher than those on the he pre-lithiation MS_2[3,28,37,41,42], we can conclude that the pre-lithiation is an effective treatment for MS_2 to achieve enhanced charge-discharge rates. The effect of Li diffusion barriers to the charge-discharge rates can be roughly estimated with the Arrhenius equation, $D \propto \exp(-E_{barrier}/k_BT)$, where $E_{barrier}$ and k_B are the Li diffusion barrier and Boltzmann constant. T is

the temperature[43]. As can be seen, the diffusion constant increases exponentially with the decreasing diffusion barrier at a constant temperature. Please note that on the three Li_2MS_2 substrates, the pre-lihtiated VS_2 monolayer is the most optimized anode material in terms of high Li binding energy and low diffusion barrier and the high Li adsorption capacity. Figure 6 summarizes the LDOS of the initial states (IS) and transition states (TS) of Li diffusion on Li_2MS_2 monolayers.

One of important factors for estimating the performance of LIB anode materials is the electric conductivity. Many pristine MS_2 are semiconductors with large band gaps, implying poor electric conductivity[44–46]. As seen, all Li_2MS_2 monolayers are conducting materials. More detailed analysis of the LDOS plots shows that when a Li ion adsorbs on the Li_2MS_2 monolayer, the electronic states of Li ions are more hybridized, indicating that the interactions between the adsorbed Li and pre-lithiating Li layer are chiefly metallic bonding. This is consisted with the previous theoretical investigates[47].

The differential charge densities were calculated in order to identify the bonding characteristics between the diffusing Li ion and the Li_2MS_2 substrates. As clearly shown in Fig. 7, the electrons are accumulated between the diffusing Li ion and the Li_2MS_2. In addition, the areas of such charge accumulations expand on three neighing Li ions in the Li_2MS_2, indicating that the accumulated electrons are delocalized. This agree well with the PDOS analysis that the interactions are metallic bonding. As a result, the migration of the diffusing Li ion does not need to break the Li-Li_2MS_2 bonds. Correspondingly, the Li diffusion barrier on Li_2MS_2 should be very small, which is in good consistence with our CI-NEB calculations.

Conclusions

In conclusion, the adsorption of Li ions on the surface of the pristine/pre-lithiated MS_2 monolayer (Li_2MS_2, M = Mo, W, V) are systematically investigated. Our calculations showed that the optimal adsorption sites of Li ions on the pristine MS_2 is the on-top site of the metal atoms. A pre-lithiating Li layer is formed when all the on-top sites are occupied by a Li ion. The pre-lithiation of MS_2 (M = W and V) will enhance the adsorption and diffusion of Li ions. Although the Li binding energy on the clean MS_2 and the pre-lithiation are not significantly different, the Li diffusion barriers on the pre-lithiated MS_2 are much less than those on the clean MS_2, implying a fast charge-discharge property. In particular, we report that the pre-lithiated VS_2 is a very promising anode materials in the Li ion barriers, due to strong Li binding interactions and negligibly small Li diffusion barriers on the Li_2VS_2. Thus, this work not only interprets the in-depth working principles of the reported pre-lithiation for MoS_2, but also propose that the pre-lithiated VS_2 may serve as one of the best anode materials in LIBs.

Received: 1 October 2019; Accepted: 5 April 2020;
Published online: 23 April 2020

References

1. Tarascon, J. M. & Armand, M. Issues and challenges facing rechargeable lithium batteries. *Nature* **414**, 359–367 (2001).
2. Li, H., Wang, Z., Chen, L. & Huang, X. Research on Advanced Materials for Li-ion Batteries. *Advanced Materials* **21**, 4593–4607 (2009).
3. Persson, K. *et al*. Lithium Diffusion in Graphitic Carbon. *Journal of Physical Chemistry Letters* **1**, 1176–1180 (2010).
4. Winter, M., Besenhard, J. O., Spahr, M. E. & Novák, P. Insertion Electrode Materials for Rechargeable Lithium Batteries. *Advanced Materials* **10**, 725–763 (1998).
5. Nishi, Y. Lithium ion secondary batteries; past 10 years and the future. *Journal of Power Sources* **100**, 101–106 (2001).
6. Kganyago, K. & Ngoepe, P. Structural and electronic properties of lithium intercalated graphite LiC6. *Physical Review B* **68**, 205111 (2003).
7. Valencia, F., Romero, A. H., Ancilotto, F. & Silvestrelli, P. L. Lithium Adsorption on Graphite from Density Functional Theory Calculations. *The Journal of Physical Chemistry B* **110**, 14832–14841 (2006).
8. Etacheri, V., Marom, R., Elazari, R., Salitra, G. & Aurbach, D. Challenges in the development of advanced Li-ion batteries: a review. *Energy Environmental Science* **4**, 3243–3262 (2011).
9. Sides, C. R. & Martin, C. R. Nanostructured Electrodes and the Low-Temperature Performance of Li-Ion Batteries. *Advanced Materials* **17**, 125–128 (2005).
10. Winter, M. & Brodd, R. J. What are batteries, fuel cells, and supercapacitors? (vol 104, pg 4245, 2003). *Chemical Reviews* **105**, 1021–1021 (2005).
11. Nicolosi, V., Chhowalla, M., Kanatzidis, M. G., Strano, M. S. & Coleman, J. N. Liquid Exfoliation of Layered Materials. *Science* **340** (2013).
12. Geim, A. K. & Grigorieva, I. V. Van der Waals heterostructures. *Nature* **499**, 419–425 (2013).
13. Koski, K. J. & Cui, Y. The New Skinny in Two-Dimensional Nanomaterials. *ACS Nano* **7**, 3739–3743 (2013).
14. Wang, Q. H., Kalantar-Zadeh, K., Kis, A., Coleman, J. N. & Strano, M. S. Electronics and optoelectronics of two-dimensional transition metal dichalcogenides. *Nature Nanotechnology* **7**, 699–712 (2012).
15. Lin, Y. & Connell, J. W. Advances in 2D boron nitride nanostructures: nanosheets, nanoribbons, nanomeshes, and hybrids with graphene. *Nanoscale* **4**, 6908–6939 (2012).
16. Seo, J.-w *et al*. Two-Dimensional Nanosheet Crystals. *Angewandte Chemie-International Edition*. **46**, 8828–8831 (2007).
17. Hwang, H., Kim, H. & Cho, J. MoS2 Nanoplates Consisting of Disordered Graphene-like Layers for High Rate Lithium Battery Anode Materials. *Nano Letters* **11**, 4826–4830 (2011).
18. Ding, S., Zhang, D., Chen, J. S. & Lou, X. W. Facile synthesis of hierarchical MoS2 microspheres composed of few-layered nanosheets and their lithium storage properties. *Nanoscale* **4**, 95–98 (2012).
19. Du, G. *et al*. Superior stability and high capacity of restacked molybdenum disulfide as anode material for lithium ion batteries. *Chemical Communications* **46**, 1106–1108 (2010).
20. Liu, H. *et al*. Highly Ordered Mesoporous MoS2 with Expanded Spacing of the (002) Crystal Plane for Ultrafast Lithium Ion Storage. *Advanced Energy Materials* **2**, 970–975 (2012).
21. Wang, Y. *et al*. Pre-lithiation of onion-like carbon/MoS2 nano-urchin anodes for high-performance rechargeable lithium ion batteries. *Nanoscale* **6**, 8884–8890 (2014).
22. Kresse, G. & Hafner, J. Ab initio molecular dynamics for liquid metals. *Physical Review B* **47**, 558–561 (1993).
23. Kresse, G. & Joubert, D. From ultrasoft pseudopotentials to the projector augmented-wave method. *Physical Review B* **59**, 1758–1775 (1999).

24. Kresse, G. & Furthmüller, J. Efficient iterative schemes for ab initio total-energy calculations using a plane-wave basis set. *Physical Review B* **54**, 11169–11186 (1996).
25. Kresse, G. & Furthmuller, J. Efficiency of ab-initio total energy calculations for metals and semiconductors using a plane-wave basis set. *Computational Materials Science* **6**, 15–50 (1996).
26. Blöchl, P. E. Projector augmented-wave method. *Physical Review B* **50**, 17953–17979 (1994).
27. Perdew, J. P., Burke, K. & Ernzerhof, M. Generalized Gradient Approximation Made Simple. *Physical Review Letters* **77**, 3865–3868 (1996).
28. Jing, Y., Zhou, Z., Cabrera, C. R. & Chen, Z. Metallic VS2 Monolayer: A Promising 2D Anode Material for Lithium Ion Batteries. *Journal of Physical Chemistry C* **117**, 25409–25413 (2013).
29. Komsa, H.-P. & Krasheninnikov, A. V. Effects of confinement and environment on the electronic structure and exciton binding energy of MoS_2 from first principles. *Physical Review B* **86**, 241201 (2012).
30. Zhuang, H. L. L., Singh, A. K. & Hennig, R. G. Computational discovery of single-layer III-V materials. *Physical Review B* **87** (2013).
31. Zhu, Z. Y., Cheng, Y. C. & Schwingenschloegl, U. Giant spin-orbit-induced spin splitting in two-dimensional transition-metal dichalcogenide semiconductors. *Physical Review B* **84** (2011).
32. Liao, J., Sa, B., Zhou, J., Ahuja, R. & Sun, Z. Design of High-Efficiency Visible-Light Photocatalysts for Water Splitting: MoS2/AlN(GaN) Heterostructures. *Journal of Physical Chemistry C* **118** (2014).
33. Debbichi, L., Eriksson, O. & Lebegue, S. Electronic structure of two-dimensional transition metal dichalcogenide bilayers from ab initio theory. *Physical Review B* **89** (2014).
34. Henkelman, G., Uberuaga, B. P. & Jónsson, H. A climbing image nudged elastic band method for finding saddle points and minimum energy paths. *Journal of Chemical Physics* **113**, 9901–9904 (2000).
35. Olsen, R. A., Kroes, G. J., Henkelman, G., Arnaldsson, A. & Jónsson, H. Comparison of methods for finding saddle points without knowledge of the final states. *Journal of Chemical Physics* **121**, 9776–9792 (2004).
36. Henkelman, G. & Jónsson, H. Improved tangent estimate in the nudged elastic band method for finding minimum energy paths and saddle points. *Journal of Chemical Physics* **113**, 9978–9985 (2000).
37. Wang, D., Liu, L.-M., Zhao, S.-J., Hu, Z.-Y. & Liu, H. Potential Application of Metal Dichalcogenides Double-Layered Heterostructures as Anode Materials for Li-Ion Batteries. *Journal of Physical Chemistry C* **120**, 4779–4788 (2016).
38. Juan, H. *et al*. First-Principles Calculation of Lithium Adsorption and Diffusion on Silicene. *Chinese Physics Letters* **30**, 17103–17106(17104) (2013).
39. Kang, B. & Ceder, G. Battery materials for ultrafast charging and discharging. *Nature* **458**, 190–193 (2009).
40. Vineyard, G. H. Frequency factors and isotope effects in solid state rate processes. *Journal of Physics and Chemistry of Solids* **3**, 121–127 (1957).
41. Persson, K., Hinuma, Y., Meng, Y. S., Van der Ven, A. & Ceder, G. Thermodynamic and kinetic properties of the Li-graphite system from first-principles calculations. *Physical Review B* **82** (2010).
42. Ling, C. & Mizuno, F. Capture Lithium in αMnO_2: Insights from First Principles. *Chemistry of Materials* **24** (2012).
43. Li, H. *et al*. MoS2/Graphene Hybrid Nanoflowers with Enhanced Electrochemical Performances as Anode for Lithium-Ion Batteries. *Journal of Physical Chemistry C* **119**, 7959–7968 (2015).
44. Li, Y., Zhou, Z., Zhang, S. & Chen, Z. MoS_2 Nanoribbons: High Stability and Unusual Electronic and Magnetic Properties. *Journal of the American Chemical Society* **130**, 16739–16744 (2008).
45. Li, Y., Wu, D., Zhou, Z., Cabrera, C. R. & Chen, Z. Enhanced Li Adsorption and Diffusion on MoS2 Zigzag Nanoribbons by Edge Effects: A Computational Study. *The Journal of Physical Chemistry Letters* **3**, 2221–2227 (2012).
46. Mak, K. F., Lee, C., Hone, J., Shan, J. & Heinz, T. F. Atomically Thin MoS2: A New Direct-Gap Semiconductor. *Physical Review Letters* **105**, 136805 (2010).
47. Xie, Y. *et al*. Prediction and Characterization of MXene Nanosheet Anodes for Non-Lithium-Ion Batteries. *Acs Nano* **8**, 9606–9615 (2014).

Acknowledgements

The work is supported by the National Key R&D Program of China (Grants No. 2017YFB0701600 and 2017YFA0204800), National Natural Science Foundation of China (Grant No. 21771134, 51761145013, 21673149), the Collaborative Innovation Center of Suzhou Nano Science & Technology, the Priority Academic Program Development of Jiangsu Higher Education Institutions (PAPD), the 111 Project and the Joint International Research Laboratory of Carbon-Based Functional Materials and Devices.

Author contributions

H.L. and Y.L. conceived the main idea. T.L., Z. J., D.L., C.D. and L.W. performed all the calculation work. All authors analyzed the results and wrote the paper.

Competing interests

The authors declare no competing interests.

Additional information

Correspondence and requests for materials should be addressed to H.L. or Y.L.

Reprints and permissions information is available at www.nature.com/reprints.

Publisher's note Springer Nature remains neutral with regard to jurisdictional claims in published maps and institutional affiliations.